The effect of angle of attack on turbulence interaction noise with a porous leading edge

Luke Bowen*, Alper Celik†, Mahdi Azarpeyvand‡
Faculty of Engineering, University of Bristol, BS8 1TR, UK

Michelle Fernandino Westin§
Embraer, Sáo José dos Campos, 12227-901, Brazil

The paper is concerned with the effect of angle of attack on the interaction noise between a turbulent flow and a NACA 0012 airfoil. This experimental study considers an airfoil with a porous leading edge up to 10% of the chord and compares the noise levels to a solid airfoil leading edge at a Reynolds number of $Re = 2.5 \times 10^5$. Turbulence is generated by the means of a passive grid and the direct noise measurements are performed using a microphone array. The airfoil is instrumented for both steady and unsteady wall pressure measurements. The C_p distribution over the surface of the airfoil is considered up to large geometric angles of attack for both the solid and porous leading edge cases. From far-field noise measurement, it is found that radiated sound is reduced at small geometric angles of attack at low frequencies for the porous airfoil. At higher angles of attack the C_p distribution of the porous leading edge case appears to be similar with that of a stalled airfoil, suggesting porous leading edges at higher angles of attack stall earlier than a solid airfoil.

I. Introduction

Noise pollution is becoming a major environmental concern in the quest for a more sustainable future. Turbulent flows are just one example of noise pollution that has sustained significant interest. Under the correct conditions, a body immersed in a turbulent flow can generate significant amounts of noise. Guide vanes in turbofan engines or flow straighteners in electric fan engines are utilized to increase the efficiency of the propulsion and can be a major noise source. This system can be thought of as a body in a turbulent flow.

Turbulence interaction noise is a subject that has been of large social interest for some time and historically has been well studied. Amiet [1] first proposed a model which can predict the interaction noise by first using linearized theory to calculate the aerodynamic response of the incident gust on the airfoil; then calculating the unsteady lift propagation to the acoustic far-field accounting for scattering and mean flow effects. Moreau and Rodger [2] studied the effects that angle of attack has on noise generation in turbulent flow and showed there is almost no dependency to angle of attack. Devenport et al. [3] studied the effects of real airfoils in turbulence and concluded that although angle of attack has a strong effect on the airfoil response function, it only has a small effect on noise generation. Celik et al. [4] demonstrated that the low sensitivity of the surface pressure response to the angle of attack extends to the energy spectra of lift and drag too. As turbulent inflow conditions are an important factor, this was extensively studied by Hutcheson et al. [5] consisting of a host of different inflow conditions and geometries, finding that as length scale and turbulence intensity increased this uniformly increased the spectral levels. As the geometry is an important factor in the noise generation there have been many studies subject to this [2, 3, 6–8], all finding that the airfoil geometry does in fact alter the noise generation in turbulent flow.

Flow control techniques are shown in many instances effective at reducing aerodynamically generated noise at the trailing edge, whether that be active or passive [9–16] systems. Serrations have been shown to be effective in reduction of aerodynamically generated noise at both the trailing edge and leading edge of an airfoil or flat plate [15, 17–21]. Porous materials have also been the subject of studies between the interaction of noise between a turbulent flow and the leading edge of an airfoil. Rodger et al. [22] used grid generated turbulence to measure the effect that a steel-wool filled NACA 0012 had on noise radiation and showed a maximum of 5dB of noise reduction is achievable from a

*Ph.D Student, Department of Mechanical Engineering, luke.bowen@bristol.ac.uk
†Postdoctoral Research Associate, Department of Mechanical Engineering, alper.celik@bristol.ac.uk
‡Professor of Aerodynamics and Aeroacoustics, Department of Mechanical Engineering, m.azarpeyvand@bristol.ac.uk
§Product Development Engineer, Embraer, Sáo José dos Campos, Brazil, michelle.westin@embraer.com.br

sub-optimal approach. There have been multiple studies on porous airfoils [23–25] which have highlighted the airfoil self-noise reduction that can be achieved with a porous airfoil. Geyer et al. carried out the first study on the effect of fully porous airfoils in turbulent flow [23]. The study focused on changing porous properties of airfoils to assess the acoustic benefit, a reduction in noise in most cases was found at the detriment to the overall hydrodynamic performance of the airfoil. Further works have showed the potential of porous materials for noise reduction [9, 16, 26–32], but a common conclusion is found that better understanding of the mechanisms and flow interaction is needed to optimize the implementation of porous materials for the noise abatement. An effort to address the understanding behind the flow mechanisms has had more consideration in recent years [33–37]. Zamponi et al. [34] studied a melamine foam airfoil and the effect on turbulence distortion near the airfoil leading edge. Ocker et al. [33] considered a wide range of porous structures for permeable leading edge airfoils to systematically study the effect of the porous structure on turbulence interaction noise and fan noise. Palleja-Cabre et al. [36] and Priddin et al. [38] experimentally and analytically studied a flat plate in a turbulent stream in a two part study. The flat plate had perforations downstream of the leading edge and demonstrated a noise reduction which is likely attributed to the airfoil acting as though it has a shorter chord. The analytical model was shown to be overall in line with the far-field noise trends found in the experimental study. Most studies neglect the effect of angle of attack, which could be due to the little sensitivity that turbulence interaction noise exhibits to changes in angle of attack at low angles of attack [3].

This study investigates the effect of angle of attack on the turbulence interaction noise of a solid and porous airfoil leading edge. A NACA 0012 airfoil is utilized in the study with an interchangeable leading edge and is immersed in a turbulent flow. The turbulent flow is generated by the use of a passive grid in an anecohic wind tunnel which does not affect the normal background noise of the wind tunnel. The study considers the mean pressure field of the airfoil across a range of angles of attack and the effect of the porous leading edge. Furthermore, the study considers the far-field noise measured by the facilities far-field noise array in addition to the near field noise, measured by microphones on the surface of the airfoil.

II. Measurement Setup

A. Wind tunnel and model

The experiments were performed in the University of Bristol Aeroacoustic Facility, which is a closed-circuit, open-jet anechoic wind tunnel. Figure 1 displays a schematic of the wind tunnel contraction with turbulence grid, the airfoil, and a closed-up look of the grid with definitions of the parameters. The anechoic chamber has physical dimensions of 6.7 m x 4.0 m x 3.3 m and is anecohic down to 160 Hz [39]. The contraction nozzle outlet has physical dimensions of 500 mm in width and 775 mm in height which allows for a steady operation from 5 m/s to 45 m/s and a normal turbulence intensity level below 0.2% [39]. The airfoil was a NACA 0012 profile which has a span of 600 mm and chord of 200 mm. It was manufactured in one piece using the additive manufacturing technique of Selective Laser Sintering (SLS) from polymide. It was designed to be highly instrumented for the measurement of both aerodynamic and aeroacoustic phenomena in the form of static pressure and unsteady surface pressure. Measurement was achieved by the use of brass tubes which were installed with 2 part epoxy resin and smoothed to the surface of the airfoil. In total there were 48 static pressure taps and 88 unsteady surface pressure taps which were drilled with a 0.4mm bit to avoid pressure attenuation at high frequencies. The surface pressure taps were connected in a remote sensing configuration using Panasonic WM-61A microphones [40]. All microphones were calibrated in both magnitude and phase referenced to a single GRAS 40PL microphone, which was calibrated using a GRAS 42AA pistonphone calibrator. Static pressure measurements were obtained from two Chell MicroDaq-32 pressure acquisition systems and were sampled for 32 seconds at 1000Hz.

B. Far field measurement

The turbulence interaction noise was measured using the far field microphone array. The array consists of 23 microphones arranged at 5° increments between polar angles of 40° and 150° to allow for directivity measurements. The arc was located 1.75 m above the airfoil and microphone at 90° was located directly above the leading edge of the airfoil. The microphones on the arc were 1/4 inch GRAS 40PL microphones, which exhibit a flat frequency response for a large dynamic range of 10 Hz $< f <$ 20,000 Hz. All microphones were calibrated using a GRAS 42AA pistonphone calibrator prior to the experiments.

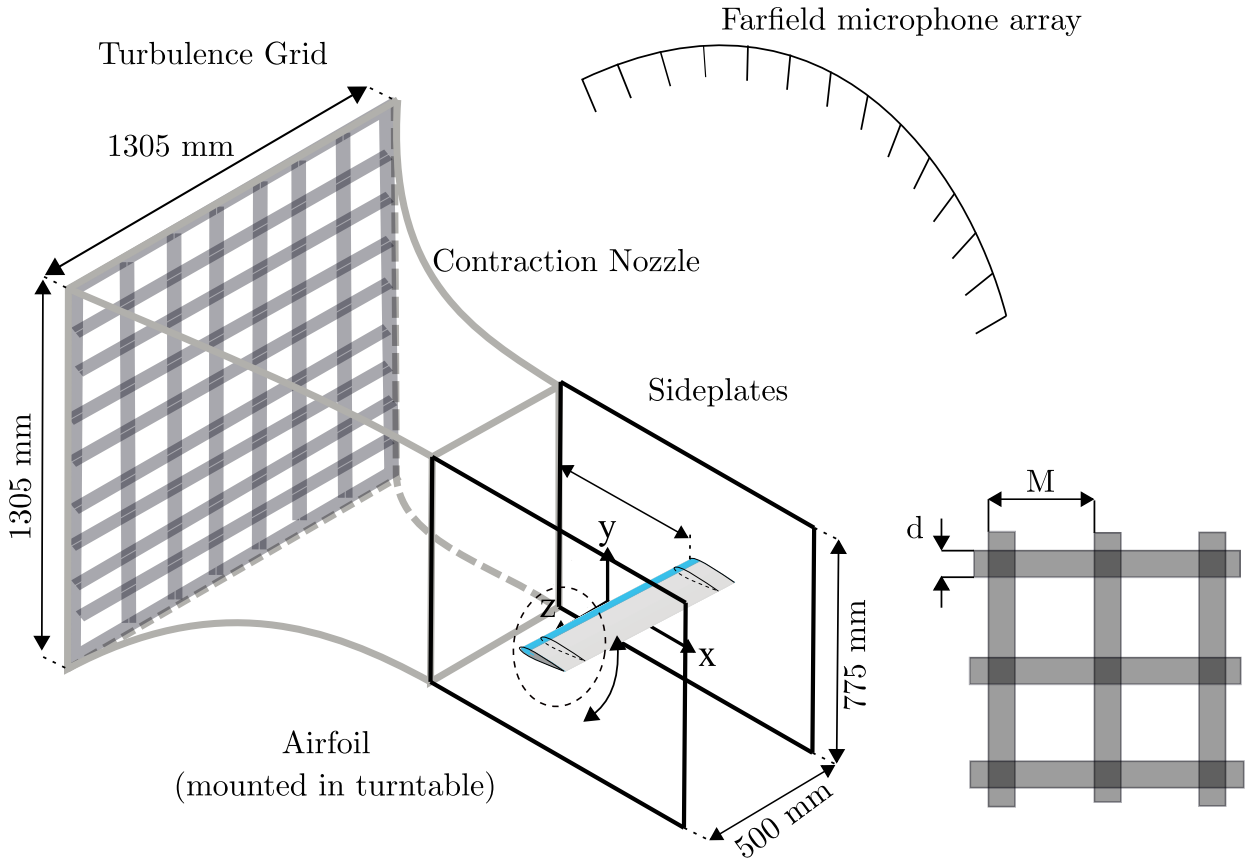

Fig. 1 Schematic of the turbulence-airfoil interaction set up in the aeroacoustic wind tunnel facility with a grid generating a turbulent inflow, a NACA 0012 airfoil with interchangeable leading edge mounted between side plates, the far field microphone array, and the details of the grid.

C. Turbulence grids

To generate the incoming turbulence, a grid was placed within the contraction nozzle of the wind tunnel. The position of the grid within the tunnel was shown to not affect the normal background jet noise of the wind tunnel [41, 42], thus allowing for direct noise measurement of the interaction noise between the turbulent flow and NACA 0012 airfoil with various porous leading edges. The geometric properties and generated flow properties of the grid are outlined in Table 1.

D. Porous leading edge

Figure 2 illustrates a schematic of the airfoil. The first 20% of the leading edge was interchangeable, between a solid, instrumented leading edge and 3D printed porous structure. A single porous leading edge was tested in order to understand the effect of angle of attack on the radiated noise. The structure is based on the Schwarz P-surface which

Table 1 The geometric properties of the grid, and the flow properties at the position of contraction nozzle exit, $x = 0$, at a freestream velocity $U_\infty = 20m/s$.

Grid	Diameter, d (mm)	Mesh, M (mm)	σ	Turbulence intensity (%)	Integral length scale (mm)
$G2$	45	233	0.35	10.1	10.8

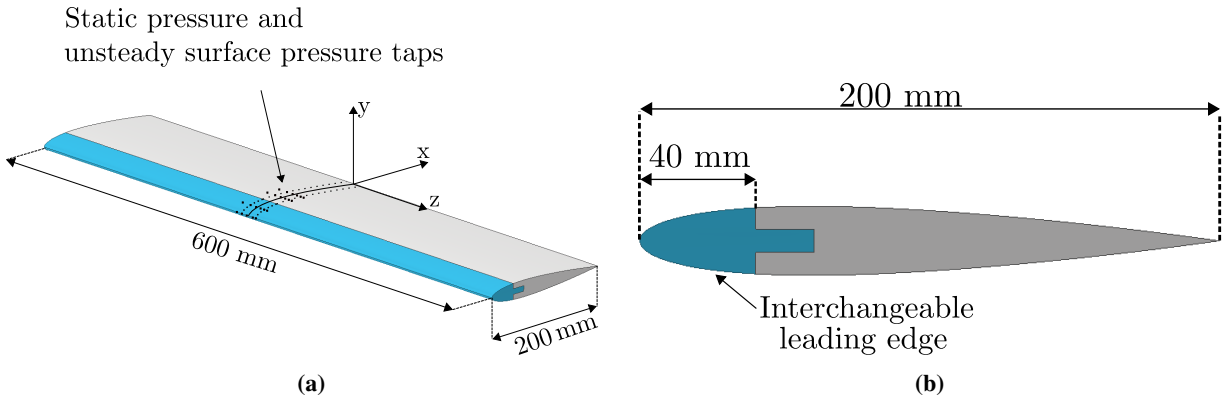

Fig. 2 Schematic of the NACA 0012 airfoil with a interchangeable leading edge, a) Isometric view showing pressure tap and unsteady surface pressure tap locations and b) side view of the airfoil showing the interchangeable part.

occupied the first 10% of the airfoil chord. The porous leading edge was printed in-house at the University of Bristol using a FormLabs Form3 stereolithography (SLA) printer. The tested structure was characterised prior to tests for both porosity and permeability, the more detailed procedure is previously presented [32]. The permeability and porosity of the structure are previously reported as $\kappa = 4.4x10^{-9}$ and 50%, respectively.

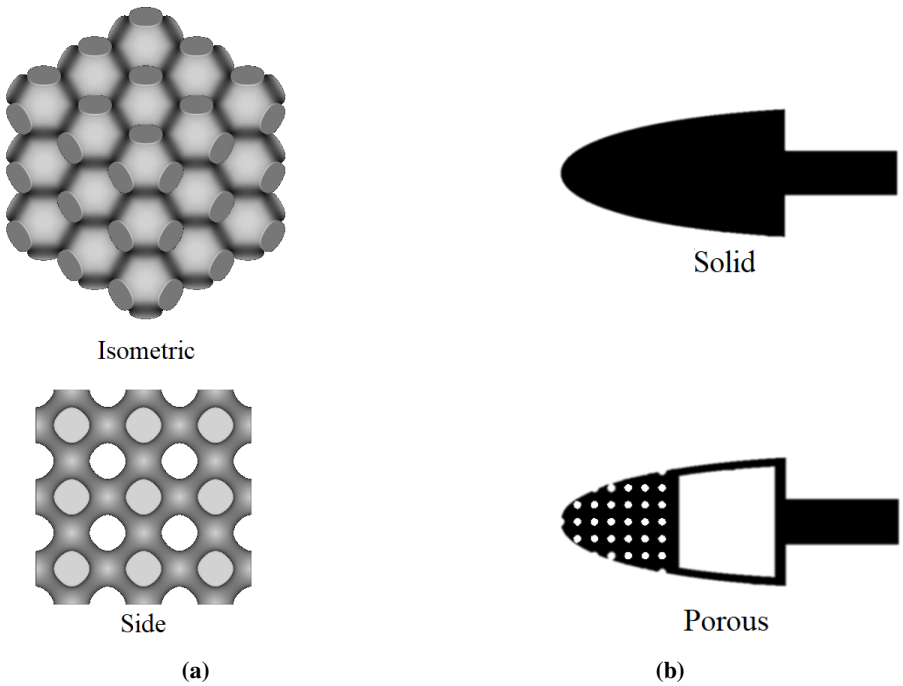

Fig. 3 Leading edges used in the experiments where (a) is the base cell of the Schwarz-P structure and (b) are the interchangeable leading edges.

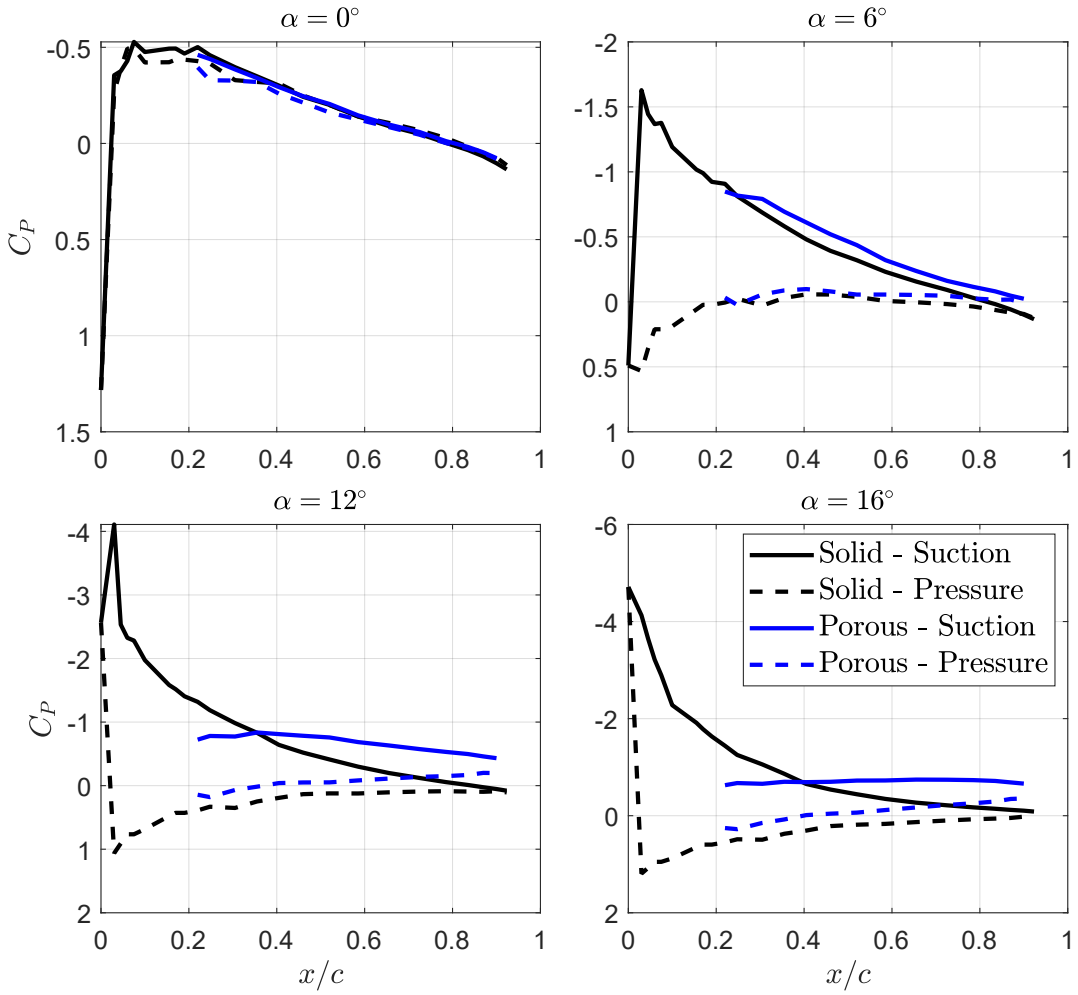

Fig. 4 Mean pressure coefficient (C_p) results for the NACA0012 airfoil with the solid leading edge compared to the porous leading edge for the angles of attack of $\alpha = 0°, 6°, 12°$ and $16°$.

III. Results and Discussion

The results comprise both the mean pressure field around the airfoil and the far-field noise followed by the near-field noise. The results of the airfoil with porous leading edge are compared to the results of the solid airfoil case in each instance.

A. Mean pressure field

The non-dimensional pressure coefficient (C_p) and the root-mean-square (rms) of the pressure coefficient value ($C_{p,rms}$) along the chord of the airfoil is calculated and presented in this section. The influence of the porous material on the suction peak that is typical of the pressure coefficient distribution over an airfoil cannot be studied due to lack of instrumentation on the leading edge of the airfoil. However, the influence of the porous material can be assessed on the remaining chord of the airfoil that is instrumented. In this case we consider the effect of the porous leading edge on the chord between $0.2 < x/c < 1$.

Figure 4 presents the results of the non-dimensional pressure coefficient (C_p) for the NACA 0012 airfoil with solid leading edge, compared to the results of the airfoil with a porous leading edge for angles of attack $\alpha = 0°, 6°, 12°$ and $16°$, at a freestream velocity of $u_\infty = 20$ m/s. The C_P distribution at $\alpha = 0°$ for the solid case shows a typical pressure

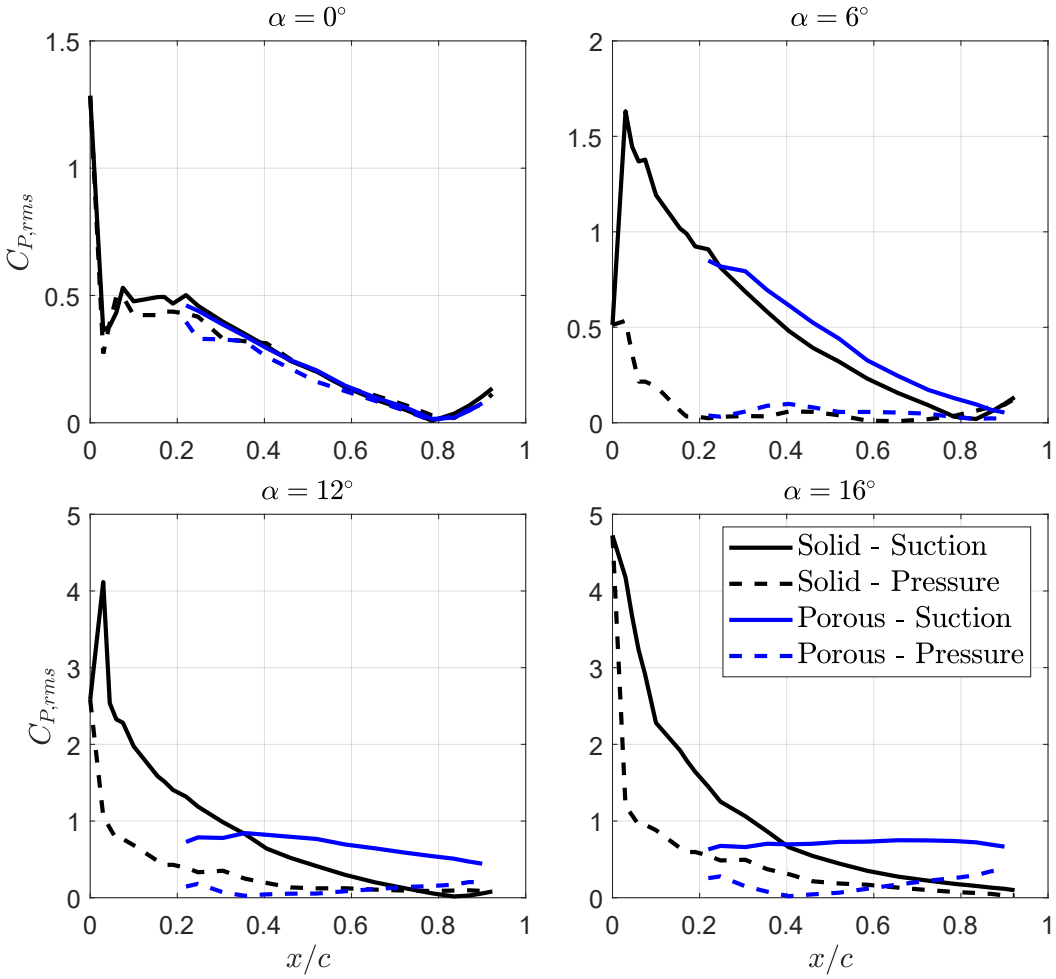

Fig. 5 Root-mean-square of the mean pressure coefficient ($C_{p,rms}$) for the NACA0012 airfoil with the solid leading edge compared to the porous leading edge for the angles of attack of $\alpha = 0°, 6°, 12°$ and $16°$.

distribution expected for a symmetric airfoil, which was previously validated against xFoil [31]. When comparing the results of the porous case to the solid airfoil case, it can be suggested that the solid part of the airfoil between $0.2 < x/c < 1$ demonstrates a comparable agreement between the two cases, for angles of attack $\alpha = 0°$ and $\alpha = 6°$. At higher angles of attack, $\alpha = 12°$ and $\alpha = 16°$, the C_P distribution shows a sharp peak at the leading edge for the solid case, which indicates an attached flow. However, for both $\alpha = 12°$ and $\alpha = 16°$, the C_P distribution for the porous leading edge case show a flat behavior, which is an indication of a stalled airfoil.

Figure 5 presents the results of the rms of the pressure coefficient ($C_{p,rms}$) for the NACA 0012 airfoil with the solid leading edge and the porous leading edge for angles of attack $\alpha = 0°, 6°, 12°$ and $16°$ at a freestream velocity of $u_\infty = 20$ m/s. The $C_{p,rms}$ results are comparable to that of the C_p results, when considering the overall trend. A good agreement is evident, between the solid and porous leading edge cases, for the results of the $C_{p,rms}$ for angles of attack $\alpha = 0°$ and $\alpha = 6°$, for the chord between $0.2 < x/c < 1$. For the results of $C_{p,rms}$ for angles $\alpha = 12°$ and $\alpha = 16°$ there appears to be a significant difference in between the solid and porous cases. This suggests there is a different behavior of the flow between the results of the two cases.

Figure 6 presents the lift curve slope for the solid leading edge case only as it is not feasible to calculate for the porous case. This C_L curve is calculated from the pressure distribution and is presented against the geometric angle of attack of the airfoil. The figure shows a linear region up to $\alpha = 16°$ at which point the airfoil is considered to stall.

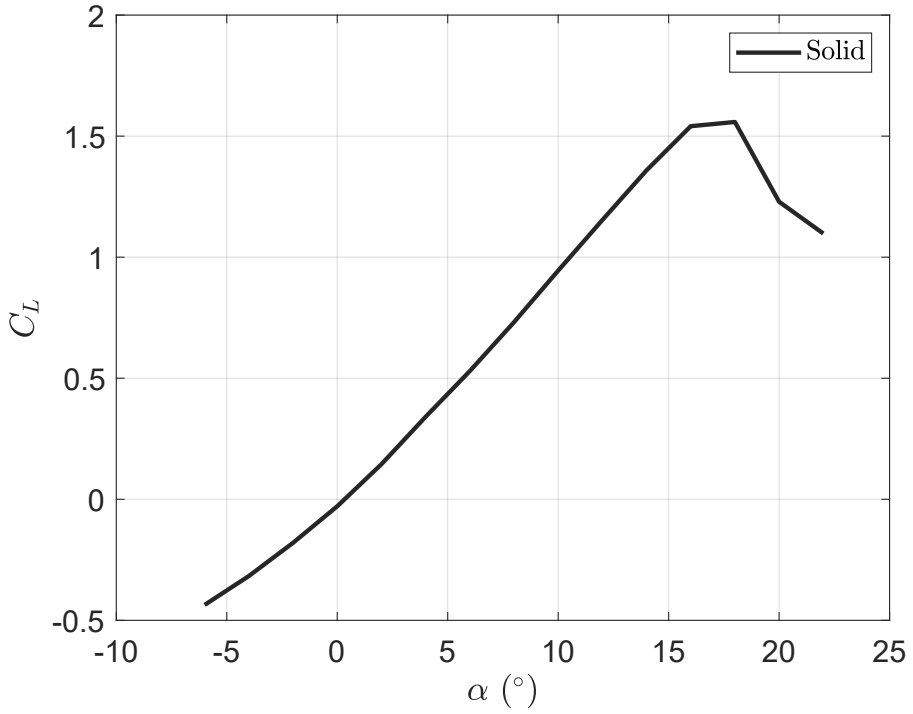

Fig. 6 Coefficient of lift against geometric angle of attack for the solid NACA 0012 airfoil.

B. Far-field analysis

The far-field noise generated by the NACA0012 airfoil with a solid leading edge and the porous leading edge immersed in the flow generated by a turbulence grid are presented in this section. The section considers the power spectral density level of the far-field noise observed at a polar angle of $\theta = 90°$ over the frequencies 160 Hz$< f < 10,000$ Hz. It is calculated using $PSD = 10 \cdot \log_{10}(\phi_{pp}/p_{ref}^2)$, where ϕ_{pp} is the power spectral density of the measured acoustic pressure and p_{ref} is the reference pressure of 20 μPa. Secondly, the overall sound pressure level (OASPL) is presented and the directivity of the OASPL is considered. The overall sound pressure level is calculated as,

$$OASPL = 10 \cdot \log_{10}\left[\frac{\int \phi_{pp}(f)df}{p_{ref}^2}\right], \tag{1}$$

integrating the energy spectrum with respect to frequency, between 160 Hz$< f < 20,000$ Hz.

Figure 7 presents the far-field narrowband spectra of the turbulence interaction noise results for the solid leading edge case in comparison to the porous case. The results are presented for the angles of attack $\alpha = 0°, 6°, 12°$ and $16°$, at a freestream velocity of $U_\infty = 20$ m/s. Considering the results of the solid leading edge, the noise peaks at low frequency (i.e. $f = 200$ Hz) and steadily decays with increasing frequency. The far-field noise results of the solid case for angles of attack $\alpha = 0°$ and $\alpha = 6°$ show similar trend, although there is an increase at high frequencies above $f > 6000$ Hz for higher angles of attack. At the angles of attack of $\alpha = 12°$ and $\alpha = 16°$, the interaction noise generated by the solid leading edge appears to slightly increase compared to the results of the lower angles of attack presented. From the inspection of Fig. 7 it can be seen that the results of the porous leading edge spectra show a reduction compared to the results of the solid case for each angle of attack for frequencies less than $f < 1000$ Hz. At $\alpha = 0°$, the noise reduction is considerably less compared to the results of the other angles that are presented. Interestingly, the high frequency noise increase in the results of the porous case are comparable across all the presented angles, suggesting there is little sensitivity to angle of attack for the noise increase. The results for $\alpha = 16°$ show the largest difference between the noise generated by the solid and porous leading edges.

Figure 8 presents the results of the difference between the noise generated by the solid leading edge with the results of the porous leading edge subtracted as $\Delta PSD = PSD_{solid} - PSD_{porous}$. It is worth noting that a positive ΔPSD

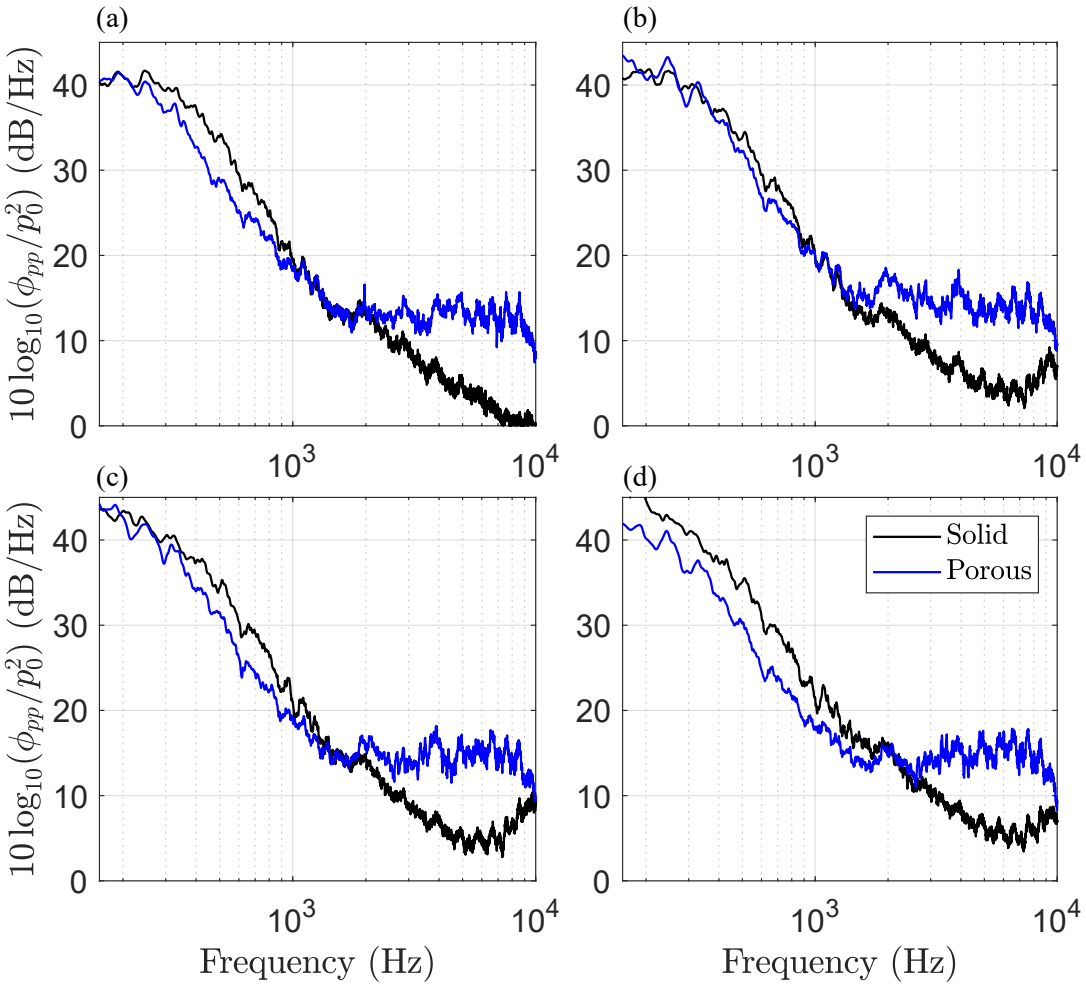

Fig. 7 Narrowband far-field noise generated by the NACA 0012 airfoil with solid and porous leading edges at angles of attack $\alpha = 0°, 6°, 12°$ and $16°$.

value denotes a noise reduction, and a negative value denotes a noise increase. The contour plot in Fig. 8 presents the *PSD* level across the frequency range 160 Hz$< f < 10,000$ Hz for the angles of attack between $-6° < \alpha < 26°$. Inspection of the figure reveals an apparent noise reduction at low frequencies and a noise increase at higher frequencies. These observations are consistent with the studies in turbulence interaction noise with a porous leading edge [**?**]. There are two main areas of significant noise reduction in the results centered around angles of attack of $\alpha = 0°$ and $\alpha = 16°$. Noise reduction centered around angle of attack $\alpha = 0°$ suggests that the porous leading edge works most optimally for zero lift condition on this symmetric airfoil. The noise reduction centered around $\alpha = 16°$ could be due to a fundamental change to the airflow characteristics at higher angles of attack, as shown in Fig. 4.

Figure 9 presents the results of the overall sound pressure level directivity of the noise for the solid and the porous leading edge cases, for angles of attack of $\alpha = 0°, 6°, 12°$ and $16°$, at a freestream velocity of $U_\infty = 20$ m/s. The overall sound pressure level takes into account the full frequency spectrum and accounts for the noise reduction at low frequency and increase at higher frequency which is evident in the porous leading edge results. The results at $\alpha = 0°$ show a significant reduction for the porous leading edge compared to the solid leading edge, for all the angles presented. Noise reduction is more evident for directivity angles of $\theta < 90°$. As the angle of attack increases, $\alpha = 6°$, the level and directivity of the noise generated by the solid leading edge and the porous leading edge appear to be comparable. Furthermore, there are no changes to the directivity of the radiated noise. As the angle increases to $\alpha = 12°$ and $\alpha = 16°$ there is a reduction in the OASPL for the porous case, compared with the solid airfoil. This is a two-fold effect, as the

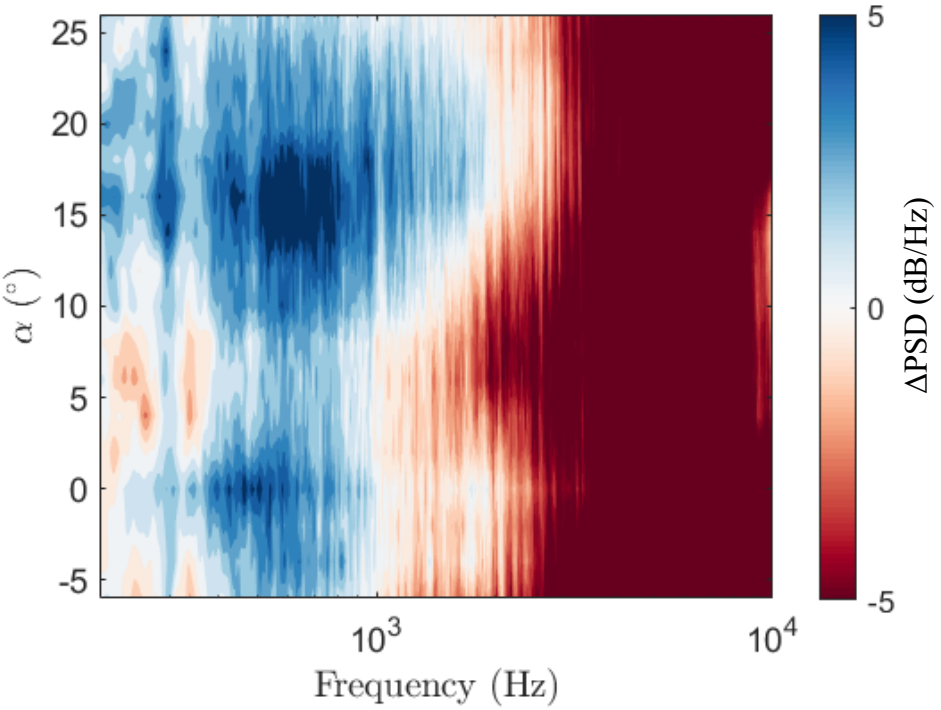

Fig. 8 Contour plot of ΔPSD far-field noise between the solid and porous case for all tested angles of attack

OASPL of the solid case increases with increasing angle of attack coupled with a further reduction in the OASPL results of the porous case.

Figure 10 presents the overall sound pressure level measured by the far-field microphone at $\theta = 90°$ against the angle of attack for both the solid leading edge and the porous leading edge at a freestream velocity of $U_\infty = 20$ m/s. This figure is quite revealing as it considers the overall sound of the full spectrum at all angles of attack for each case. Considering the results of the solid leading edge, it is evident that for low geometric angles of attack, the level of far-field noise is consistent, as shown in the literature [3]. As the geometric angle of attack increases to $\alpha = 8°$, an increase in the OASPL level is evident. The OASPL continues to increase up to $\alpha = 16°$, and for angles higher than $\alpha > 16°$, the OASPL level falls significantly with a sharp decay, coinciding with the suggested stall region in Fig. 6. The porous leading edge results exhibit a more significant reduction against the solid case at $\alpha = 0°$, for the low angles of attack. Between the angles to $0° < \alpha < 6°$, the OASPL appears to increase for the porous leading edge, whereas the solid leading edge shows no discernible increase. Above $\alpha = 6°$, the OASPL results of the solid case increase up to $\alpha = 16°$, whereas the results of the porous case reduce, causing an increased difference between the OASPL results of the two cases. From the results in Fig. 4 and Fig. 5, it can be suggested that the airfoil with the porous leading edge may have stalled for angles above $\alpha = 6°$, which could be attributed to the reduction of interaction noise for higher angles of attack. At $\alpha = 26°$ the OASPL results are comparable between the two leading edges.

C. Near-field analysis

The near field analysis is considered in the following section. As with the pressure coefficient results, it is not possible to compare the porous section of the airfoil with the solid airfoil due to lack of instrumentation over the porous structure on the leading edge. However, it is possible to compare the immediate downstream effects, and the remainder of the solid part of the airfoil to the trailing edge. The surface pressure fluctuations in chordwise region between $0.24 < x/c < 0.92$ is considered in this section, and the results are displayed as the power spectral density of the surface pressure fluctuation at multiple locations over the solid part of the airfoil.

Figure 11 presents the results of the PSD level of the unsteady surface pressure fluctuations for both the solid and porous leading edges, for angles of attack $\alpha = 0°, 6°, 12°$ and $16°$ at chordwise locations of $x/c = 0.25, 0.52$ and 0.92.

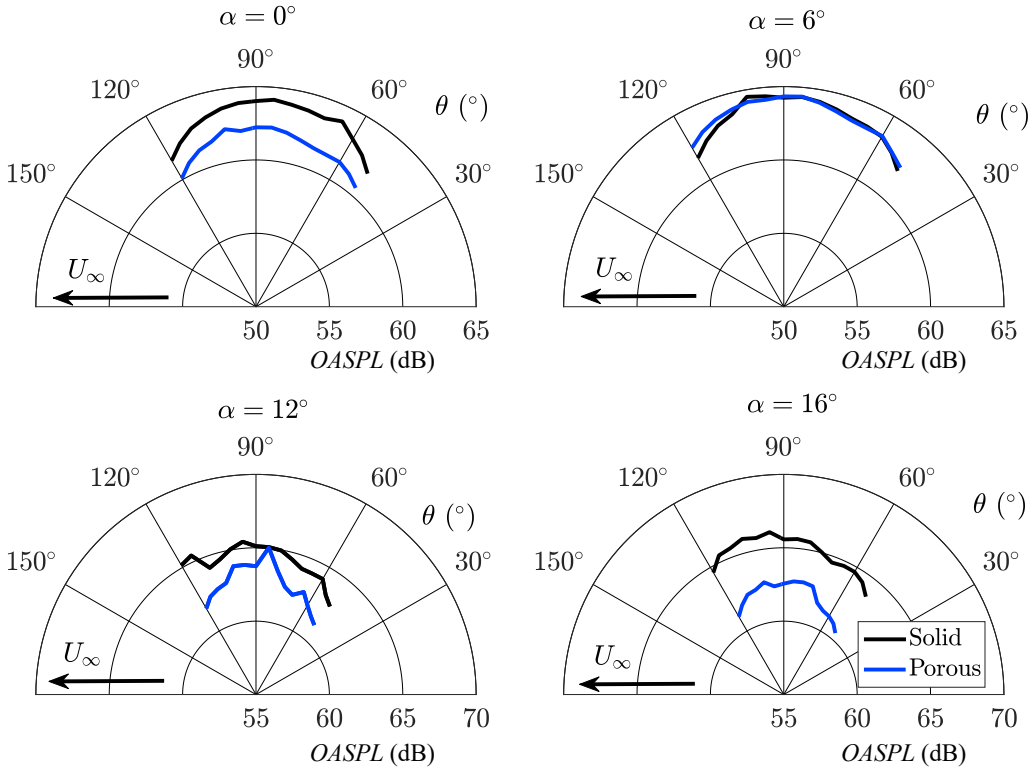

Fig. 9 Overall sound pressure level directivity results for the NACA0012 airfoil with the solid leading edge compared to the porous leading edge for the angles of attack of $\alpha = 0°, 6°, 12°$ and $16°$.

For the angle of attack $\alpha = 0°$, the surface pressure fluctuation level is comparable between the solid and porous cases, with the porous case increasing at frequencies $f < 1000$ Hz at chordwise locations $x/c = 0.52$ and $x/c = 0.92$. For the angles of attack of $\alpha = 6°$ and $\alpha = 12°$, the low and high frequency of the surface pressure fluctuations are very different at $x/c = 0.24$. Further downstream at $x/c = 0.52$ and $x/c = 0.92$, for the same angles the high frequency behavior of the surface pressure fluctuation is comparable between the cases, i.e. $f > 1500$ Hz. At $\alpha = 16°$, the results of the porous leading edge unsteady surface pressure are significantly less than the solid results at $x/c = 0.24$, suggesting a large reduction in the unsteady surface pressure fluctuations when compared to the solid leading edge results. However, further downstream at the trailing edge the results between the porous and solid leading edge are comparable.

IV. Conclusion

This paper considers the effect of a porous leading edge on the interaction noise generated at a range of angles of attack. The pressure coefficient distribution suggests that the pressure distribution across the solid part of the airfoil at small angles of attack is comparable between the solid and porous cases. The noise reduction due to the porous leading edge appears to be most effective at zero angle of attack, and the noise reduction diminishes as the angle of attack increases. The directivity of the turbulence interaction noise at low angles of attack is mainly unchanged, despite a reduction in the OASPL results for the porous leading edge case. At high geometric angles of attack, the flat C_p distribution over the solid part of the airfoil for the porous leading edge case indicates a premature stall on the airfoil. The noise reduction due to the porous leading edge appears to be significant at higher angles of attack, due to a combination of a reduction in turbulence interaction noise due to the stalled airfoil coupled with noise increase in the solid case due to separation noise. Whereas for the same increase in angle of attack a further noise reduction is seen in the porous case. As the C_p distribution suggests the possibility of a premature stall in the porous case, it can be

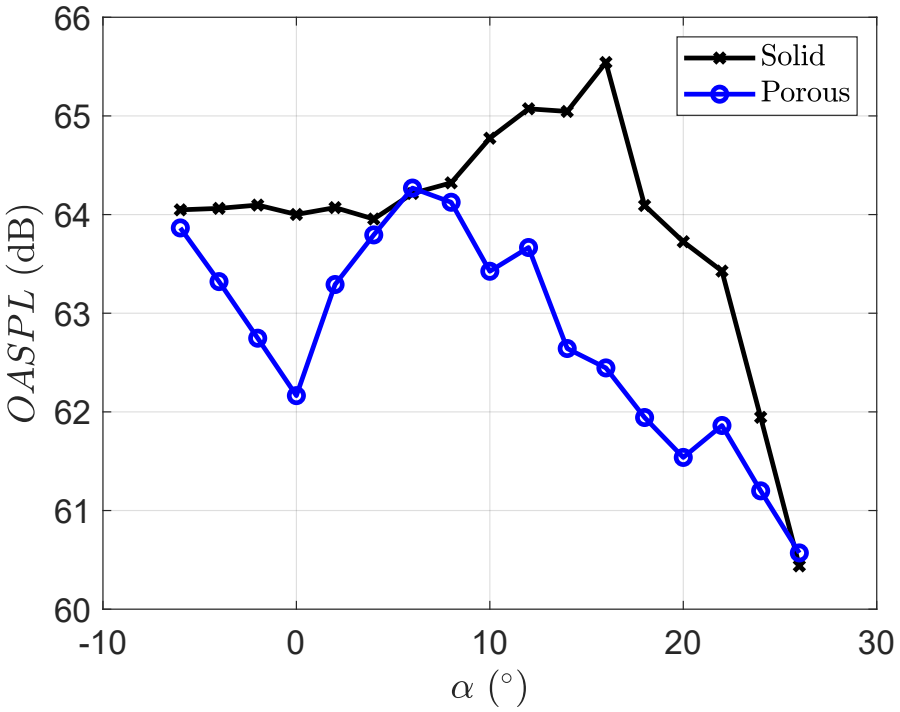

Fig. 10 Overall sound pressure level measured at the $\theta = 90^\circ$ microphone for the solid and porous leading edge cases for all angles of attack.

suggested that the noise reduction at higher angles is not strictly valid due to a change in aerodynamic noise generation mechanism. Analysis of the surface pressure fluctuations shows significantly different behavior to the PSD of surface pressure fluctuations between the solid and porous leading edge cases. The most significant differences are observed closer to the leading edge region on the airfoil surface.

Acknowledgments

The first author (L.B.) would like to acknowledge the financial support of Embraer S.A. and EPSRC (Engineering and Physical Sciences Research Council) via Grant No. EP/S013024/1 *"Aerodynamics and aeroacoustics of turbulent flows over and past permeable rough surfaces"*.

References

[1] Amiet, R., "Acoustic radiation from an airfoil in a turbulent stream," *Journal of Sound and Vibration*, Vol. 41, No. 4, 1975, pp. 407 – 420. https://doi.org/https://doi.org/10.1016/S0022-460X(75)80105-2.

[2] Moreau, S., and Roger, M., "Effect of Angle of Attack and Airfoil Shape on Turbulence-Interaction Noise," 11th AIAA/CEAS Aeroacoustics Conference, Monterey, CA, AIAA-2005-2973, 2005.

[3] Devenport, W. J., Staubs, J. K., and Glegg, S. A., "Sound radiation from real airfoils in turbulence," *Journal of Sound and Vibration*, Vol. 329, No. 17, 2010, pp. 3470 – 3483. https://doi.org/https://doi.org/10.1016/j.jsv.2010.02.022.

[4] Celik, A., Bowen, L., and Azarpeyvand, M., "Unsteady aerodynamic response of a NACA0012 in smooth and turbulent flows," AIAA AVIATION 2020 FORUM, AIAA-2020-2600, 2020.

[5] Hutcheson, F. V., Brooks, T. F., and Stead, D. J., "Measurement of the Noise Resulting from the Interaction of Turbulence with a Lifting Surface," *International Journal of Aeroacoustics*, Vol. 11, No. 5-6, 2012, pp. 675–700. https://doi.org/10.1260/1475-472X.11.5-6.675.

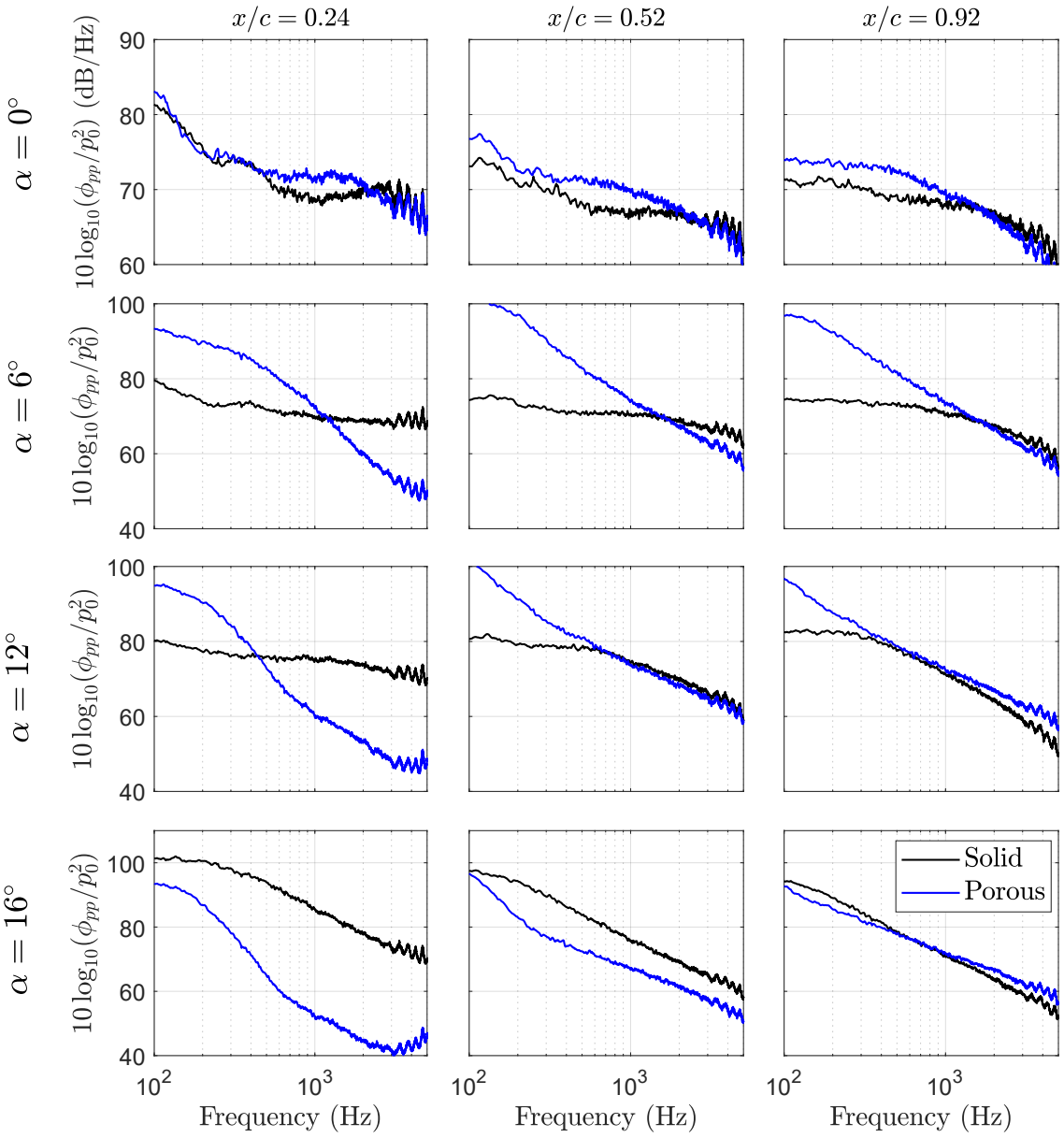

Fig. 11 PSD of surface pressure fluctuation results for the NACA0012 airfoil with the solid leading edge compared to the porous leading edge for the angles of attack of $\alpha = 0°, 6°, 12°$ and $16°$ at three chordwise locations of $x/c = 0.24, 0.52$ and 0.92.

[6] Gill, J., Zhang, X., and Joseph, P., "Symmetric airfoil geometry effects on leading edge noise," *The Journal of the Acoustical Society of America*, Vol. 134, No. 4, 2013, pp. 2669–2680. https://doi.org/10.1121/1.4818769.

[7] Gill, J. R., Zhang, X., and Joseph, P., "Effects of Real Airfoil Geometry on Leading Edge Gust Interaction Noise," 19th AIAA/CEAS Aeroacoustics Conference, Berlin, Germany AIAA-2013-2203, 2013. https://doi.org/10.2514/6.2013-2203.

[8] Gershfeld, J., "Leading edge noise from thick foils in turbulent flows," *The Journal of the Acoustical Society of America*, Vol. 116, No. 3, 2004, pp. 1416–1426. https://doi.org/10.1121/1.1780575.

[9] Showkat Ali, S. A., Azarpeyvand, M., and Ilário da Silva, C. R., "Trailing-edge flow and noise control using porous treatments," *Journal of Fluid Mechanics*, Vol. 850, 2018, pp. 83–119. https://doi.org/10.1017/jfm.2018.430.

[10] Showkat Ali, S. A., Azarpeyvand, M., Szőke, M., and Ilário da Silva, C. R., "Boundary layer flow interaction with a permeable wall," *Physics of Fluids*, Vol. 30, No. 8, 2018, p. 085111. https://doi.org/10.1063/1.5043276.

[11] Showkat Ali, S. A., Azarpeyvand, M., and da Silva], C. R. I., "Trailing edge bluntness noise reduction using porous treatments," *Journal of Sound and Vibration*, Vol. 474, 2020, p. 115257. https://doi.org/https://doi.org/10.1016/j.jsv.2020.115257.

[12] Liu, X., Jawahar, H. K., Azarpeyvand, M., and Theunissen, R., "Aerodynamic Performance and Wake Development of Airfoils with Serrated Trailing-Edges," *AIAA Journal*, Vol. 55, No. 11, 2017, pp. 3669–3680.

[13] Mayer, Y. D., Lyu, B., Jawahar, H. K., and Azarpeyvand, M., "A semi-analytical noise prediction model for airfoils with serrated trailing edges," *Renewable Energy*, Vol. 143, 2019, pp. 679 – 691. https://doi.org/https://doi.org/10.1016/j.renene.2019.04.132.

[14] Jawahar, H. K., Ai, Q., and Azarpeyvand, M., "Experimental and numerical investigation of aerodynamic performance for airfoils with morphed trailing edges," *Renewable Energy*, Vol. 127, 2018, pp. 355 – 367. https://doi.org/https://doi.org/10.1016/j.renene.2018.04.066.

[15] Celik, A., Mayer, Y., and Azarpeyvand, M., "An Experimental Aeroacoustic Study on Serrated Trailing-Edge Geometries and Flow Misalignment Effects," AIAA AVIATION 2020 FORUM, AIAA-2020-2518, 2020.

[16] Carpio, A. R., Avallone, F., and Ragni, D., "On the Role of the Flow Permeability of Metal Foams on Trailing Edge Noise Reduction," 2018 AIAA/CEAS Aeroacoustics Conference, Atlanta, GA, AIAA-2018-2964, 2018.

[17] Lyu, B., Azarpeyvand, M., and Sinayoko, S., "Noise Prediction for Serrated Leading-edges," 22nd AIAA/CEAS Aeroacoustics Conference, Lyon, France, AIAA-2016-2740, 2016.

[18] Lyu, B., and Azarpeyvand, M., "On the noise prediction for serrated leading edges," *Journal of Fluid Mechanics*, Vol. 826, 2017, p. 205–234. https://doi.org/10.1017/jfm.2017.429.

[19] Kim, J., Haeri, S., and Joseph, P., "On the reduction of aerofoil-turbulence interaction noise associated with wavy leading edges," *Journal of Fluid Mechanics*, Vol. 792, 2016, pp. 526–552. Data files are made available from http://dx.doi.org/10.5258/SOTON/397245 as required by EPSRC Research Data Policy.

[20] Narayanan, S., Chaitanya, P., Haeri, S., Joseph, P., Kim, J. W., and Polacsek, C., "Airfoil noise reductions through leading edge serrations," *Physics of Fluids*, Vol. 27, No. 2, 2015, p. 025109. https://doi.org/10.1063/1.4907798.

[21] Chaitanya, P., Joseph, P., Narayanan, S., Vanderwel, C., Turner, J., Kim, J. W., and Ganapathisubramani, B., "Performance and mechanism of sinusoidal leading edge serrations for the reduction of turbulenceaerofoil interaction noise," *Journal of Fluid Mechanics*, Vol. 818, 2017, pp. 435–464. https://doi.org/10.1017/jfm.2017.141.

[22] Roger, M., Schram, C., and Santana, L. D., "Reduction of Airfoil Turbulence-Impingement Noise by Means of Leading-Edge Serrations and/or Porous Material," 19th AIAA/CEAS Aeroacoustics Conference, Berlin, Germany, AIAA-2013-2108, 2013.

[23] Geyer, T., Sarradj, E., Giesler, J., and Hobracht, M., "Experimental assessment of the noise generated at the leading edge of porous airfoils using microphone array techniques," 17th AIAA/CEAS Aeroacoustics Conference (32nd AIAA Aeroacoustics Conference), Portland, OR, AIAA-2011-2713, 2011.

[24] Geyer, T., Sarradj, E., and Giesler, J., "Application of a Beamforming Technique to the Measurement of Airfoil Leading Edge Noise," *Advances in Acoustics and Vibration*, Vol. 2012, 2012, pp. 1–16. https://doi.org/10.1155/2012/905461.

[25] Sarradj, E., and Geyer, T., "Noise Generation by Porous Airfoils," 13th AIAA/CEAS Aeroacoustics Conference (28th AIAA Aeroacoustics Conference), AIAA-2007-3719, 2007.

[26] Geyer, T. F., Lucius, A., Schrödter, M., Schneider, M., and Sarradj, E., "Reduction of Turbulence Interaction Noise Through Airfoils With Perforated Leading Edges," *Acta Acustica united with Acustica*, Vol. 105, No. 1, 2019, pp. 109–122. https://doi.org/doi:10.3813/AAA.919292.

[27] Roger, M., Schram, C., and Santana, L. D., "Reduction of Airfoil Turbulence-Impingement Noise by Means of Leading-Edge Serrations and/or Porous Material," 19th AIAA/CEAS Aeroacoustics Conference, Berlin, Germany AIAA-2013-2108, 2013.

[28] Sinnige, T., Corte, B. D., De Vries, R., Avallone, F., Merino-Martínez, R., Ragni, D., Eitelberg, G., and Veldhuis, L. L. M., "Alleviation of Propeller-Slipstream-Induced Unsteady Pylon Loading by a Flow-Permeable Leading Edge," *Journal of Aircraft*, Vol. 56, No. 3, 2019, pp. 1214–1230. https://doi.org/10.2514/1.C035250.

[29] Geyer, T. F., "Measurement of the turbulence interaction noise generated by flat plates with perforated leading edges," AIAA AVIATION 2020 FORUM, AIAA-2020-2576, 2020.

[30] Bampanis, G., and Roger, M., "On the Turbulence-Impingement Noise of a NACA-12 Airfoil with Porous Inclusions," AIAA AVIATION 2020 FORUM, AIAA-2020-2577, 2020.

[31] Bowen, L., Celik, A., Azarpeyvand, M., and da Silva, C. R. I., "On the use of Tailored Permeable Surfaces for Turbulence Interaction Noise Control," AIAA AVIATION 2020 FORUM, AIAA-2020-2530, 2020.

[32] Bowen, L., Celik, A., Azarpeyvand, M., and da Silva, C. R. I., "Porous geometry effects on the generation of turbulence interaction noise," AIAA AVIATION 2021 FORUM, AIAA-2021-2193, 2021.

[33] Ocker, C., Geyer, T. F., Czwielong, F., Krömer, F., Pannert, W., Merkel, M., and Becker, S., "Permeable Leading Edges for Airfoil and Fan Noise Reduction in Disturbed Inflow," *AIAA Journal*, Vol. 59, No. 12, 2021, pp. 4969–4986. https://doi.org/10.2514/1.J060396.

[34] Zamponi, R., Satcunanathan, S., Moreau, S., Ragni, D., Meinke, M., Schröder, W., and Schram, C., "On the role of turbulence distortion on leading-edge noise reduction by means of porosity," *Journal of Sound and Vibration*, Vol. 485, 2020, p. 115561. https://doi.org/10.1016/j.jsv.2020.115561.

[35] Baddoo, P. J., Hajian, R., and Jaworski, J. W., "Unsteady aerodynamics of porous aerofoils," *Journal of Fluid Mechanics*, Vol. 913, 2021, p. A16. https://doi.org/10.1017/jfm.2020.1031.

[36] Palleja-Cabre, S., Paruchuri, C. C., Joseph, P., Priddin, M. J., and Ayton, L. J., "Downstream Perforations for the Reduction of Turbulence-Aerofoil Interaction Noise: Part I - Experimental Investigation," AIAA AVIATION 2021 FORUM, AIAA-2021-2149, 2021.

[37] Ayton, L. J., Colbrook, M., Geyer, T. F., Chaitanya, P., and Sarradj, E., "Modelling chordwise-varying porosity to reduce aerofoil-turbulence interaction noise," AIAA AVIATION 2021 FORUM, AIAA-2021-2190, 2021.

[38] Priddin, M. J., Ayton, L. J., Palleja-Cabre, S., Chaitanya, P., and Joseph, P., "Downstream Perforations for the Reduction of Turbulence-Aerofoil Interaction Noise: Part II - Theoretical Investigation," AIAA AVIATION 2021 FORUM, AIAA-2021-2147, 2021.

[39] Mayer, Y. D., Jawahar, H. K., Szőke, M., Ali, S. A. S., and Azarpeyvand, M., "Design and performance of an aeroacoustic wind tunnel facility at the University of Bristol," *Applied Acoustics*, Vol. 155, 2019, pp. 358 – 370. https://doi.org/https://doi.org/10.1016/j.apacoust.2019.06.005.

[40] Mayer, Y., Zang, B., and Azarpeyvand, M., "Near-field aeroacoustic characteristics of a stalled NACA 0012 aerofoil," *Proceedings of the 23rd International Congress on Acoustics, integrating 4th EAA Euroregio 2019*, edited by M. Ochmann, DEGA e.V., 2019, pp. 5421–5428.

[41] Bowen, L., Celik, A., Azarpeyvand, M., and da Silva, C. R. I., "Design and Analysis of Turbulence Grids for Aeroacoustic Measurements," AIAA AVIATION 2020 FORUM, AIAA-2020-2525, 2020.

[42] Bowen, L., Celik, A., Azarpeyvand, M., and da Silva, C. R. I., "Grid Generated Turbulence for Aeroacoustic Facility," *AIAA Journal*, Vol. 60, No. 3, 2022, pp. 1833–1847. https://doi.org/10.2514/1.J060851.